Physics of the Solid State, 2024, Vol. 66, No. 5

06,07

Stabilization of the polar phase of potassium nitrate, embedded in a nanoporous barium titanate matrix

© S.V. Baryshnikov, A.Yu. Milinskiy

Blagoveshchensk State Pedagogical University,
Blagoveshchensk, Russia

E-mail: a.milinskiy@mail.ru

Received April 22, 2024
Revised April 22, 2024
Accepted April 24, 2024

The temperature dependences of the linear and nonlinear dielectric properties of a nanocomposite, based on porous ceramics of barium titanate $BaTiO_3$ with embedded potassium nitrate KNO_3, were obtained. It was found that potassium nitrate, embedded in pores, exhibits stabilization of the ferroelectric state at room temperature. The stabilization of the KNO_3 polar phase is explained by the presence of significant electric fields in the pores of the ceramic.

Keywords: ferroelectric, nanocomposite, potassium nitrate, phase transitions.

DOI: 10.61011/PSS.2024.05.58503.98

1. Introduction

Nanoporous materials such as mesoporous silicate matrices MCM-41, SBA-15, porous glasses, artificial opals, aluminum oxide films are widely used on various research and development area thanks to their unique properties [1–3]. The above mentioned materials are used to create composite structures that are of interest on both practical and theoretical grounds This is associated with accurate sizing and spatial configuring of incapsulated particles by varying the pore geometry and structure. Such approach makes it possible to achieve materials with desired properties.

Composite materials based on the matrices filled with various substances, including metals, semiconductors, superionic conductors, liquid crystals, etc., have been extensively studied over recent years opening new prospects for the development of materials with desired functional properties [4]. A special focus is made on the investigation of the properties of matrix nanocomposites based on ferroelectric compounds and their mixtures: $NaNO_2$ [5], KNO_3 [6–8], DIPAB [9], KNO_3-$NaNO_3$ [10].

Examination of dielectric properties of $BaTiO_3/KNO_3$ nanocomposite, nanoporous barium titanate ceramics filled with ferroelectric KNO_3, is described herein. The unique feature of the nanoporous ceramics addressed herein is in that it is polar, as opposed to porous glasses and opals. Therefore, significant electric fields are induced inside the pores at temperatures below the Curie point.

2. Samples and experimental procedure

At atmospheric pressure, KNO_3 depending on temperature may have three different structures, one of them is a ferroelectric one. At room temperature, KNO_3 has a rhombic structure with space group Pmcn (phase II) [11]. When the temperature grows up to 128°C, KNO_3 crystals undergo a phase transition to phase I ($R\bar{3}m$). Then, when cooling down from 180°C, phase I at 124°C transforms into polar phase III (R3m) and only at lower temperatures about 105−100°C phase III transforms into phase II that is stable at room temperature. The maximum spontaneous polarization P_s in phase III is $8-10\,\mu C\cdot cm^{-2}$ [11]. Ferroelectricity life temperature range in KNO_3 is known to be defined by the thermal history and cooling rate [12,13]. Defining the conditions at which ferroelectric KNO_3 structure remains stable at room temperature and even below is an important challenge. Expansion of the polar phase stability area by creating KNO_3-based composites and solid solutions has been reported before [14,15].

$BaTiO_3$ is a classical ferroelectric material with several equivalent P_s directions [16]. Above $T_o \approx 120°C$, $BaTiO_3$ has a perovskite type cubic structure ($Pm3m$). Below $\approx 120°C$, the structure changes to a tetragonal one ($P4mm$) and spontaneous polarization P_s equal to $18\,\mu C\cdot cm^{-2}$ occurs. Then P_s increases to $26\,\mu C\cdot cm^{-2}$ during cooling to room temperature. With further temperature decrease, $BaTiO_3$ crystals change over to a rhombic phase at approx 5°C.

It is known that when $BaTiO_3$ particles are reduced to nanosizes, reactivity grows due to an increase in active surface and, therefore, the temperature sufficient for ceramics sintering decreases [17]. To achieve porous ceramics, we used $BaTiO_3$ nanopowders made by Mann Grain Nano Technology Co., Ltd. (PRC) with a mean particle size of 50 nm. The workpieces were pressed at (20 Pa) $500\,kg\cdot cm^{-2}$. A suspension consisting of polystyrene balls 100 nm in diameter made by Rigor Science Co., Ltd. (PRC) was used as an additive. After pressing, the workpieces

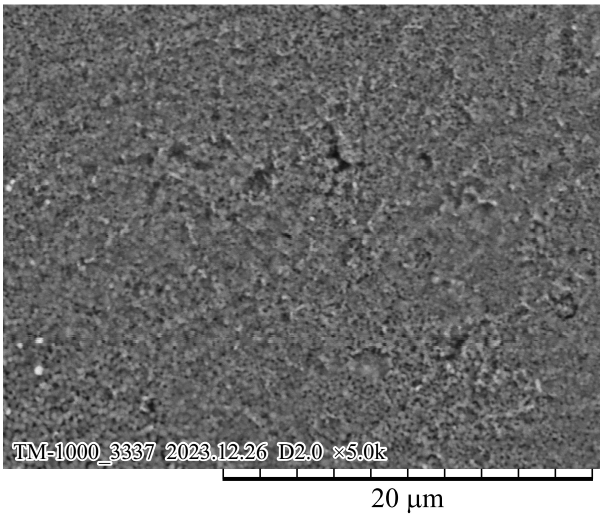

Figure 1. Electronic photograph of $BaTiO_3$ ceramics surface.

were 10 mm in diameter and 1.5 mm in thickness. The ceramics has porous structure at a sintering temperature of 1000°C. Porosity defined from the density of ceramics is equal to 15%. The electronic photograph of the ceramics is shown in Figure 1. The mean diameter of nanopores is about 150 nm.

To produce $BaTiO_3/KNO_3$ nanocomposites, the porous $BaTiO_3$ ceramics was placed in a saturated KNO_3 aqueous solution with a temperature of 100°C. Then, the solution was slowly cooled down to room temperature and held until complete water evaporation. To increase the degree of filling, the procedure was repeated. The ratio of matrix volume to KNO_3 volume determined by the change in the porous ceramics mass was equal to $\approx 9/1$. Before measurements, the prepared sample was held at 120°C during 30 to remove any water trapped in pores.

In–Ga eutectic was used as electrodes for all test samples used in the study. To examine temperature dependences $\varepsilon'(T)$, E7–25 LCR meter was used. The temperature was recorded using AOIP TC 6621 electronic thermometer. The measurements were performed within 20–180°C at a rate of 1°C/min.

To determine the polar phase life region, the nonlinear dielectric spectroscopy (NDS) method was used. In a nonlinear crystal, electric induction D may be expanded as series in powers of field strength E [18]:

$$D = P_s + \frac{\partial P}{\partial E}E + \frac{1}{2}\frac{\partial^2 P}{\partial E^2}E^2 + \frac{1}{6}\frac{\partial^3 P}{\partial E^3}E^3 + \ldots + \frac{1}{n!}\frac{\partial^n P}{\partial E^n}E^n$$

$$= P_s + \varepsilon_1 E + \varepsilon_2 E^2 + \varepsilon_3 E^3 \ldots \quad (1)$$

When $E = E_o\cos(\omega t)$ is applied to the ferroelectric material, the current will contain higher harmonics $I_{2\omega}$, $I_{3\omega}$, $I_{4\omega}$, ..., whose amplitudes are defined by nonlinear permittivities ε_2, ε_3, ε_4 ..., respectively. According to [19], currents of the corresponding harmonics will be defined as

$$I_{2\omega} = -\left[\omega S\frac{U_0^2}{h^2}\sin(2\omega t)\right.$$
$$\left.\times\left\{\chi^3\left(3\beta P_s + 10\gamma P_s^3\right) + 15\gamma P_s\chi^5\frac{U_0^2}{h^2}\right\}\right], \quad (3)$$

$$I_{3\omega} = 3\chi^4\omega S\frac{U_o^3}{h^3}\cos(3\omega t)\left\{\beta + 10\gamma P_s^2\right\}$$
$$+ \frac{15}{2}\omega S\frac{U_o^5}{h^5}\gamma\chi^6\cos(3\omega t), \quad (4)$$

$$I_{4\omega} = 15\omega S\frac{U_o^4}{h^4}\gamma P_s\chi^5\sin(4\omega t), \quad (5)$$

where U_o i s the voltage amplitude on the sample, h is the sample thickness, χ is the dielectric susceptibility, β and γ are the Landau–Ginzburg expansion coefficients.

According to (3)–(5), $I_{3\omega}$ shall grow on the approach to the Curie point in the ferroelectric phase, and then shall have its valley in the phase transition point. The harmonic amplitudes are proportional to the spontaneous polarization and, thus, the ferroelectric phase life region may be determined. This study used the second and third harmonic factors to describe nonlinearity of the samples — $\gamma_{2\omega} = I_{2\omega}/I_\omega$ and $\gamma_{3\omega} = I_{3\omega}/I_\omega$, respectively.

3. Experimental findings and discussion

Figure 2 shows the temperature trend of permittivity $\varepsilon'(T)$ and third harmonic factor $\gamma_{3\omega}(T)$ for bulk KNO_3. The maximum permittivity ε' is ≈ 20, maximum $\gamma_{3\omega}$ – 0.06 is 0.06. The polar phase according to $\gamma_{3\omega}(T)$ curve occurs only in cooling within 122–105°C.

Figure 3 shows the temperature dependences of permittivity $\varepsilon'(T)$ and second harmonic $\gamma_{2\omega}(T)$ and third harmonic $\gamma_{3\omega}(T)$ factors for porous $BaTiO_3$ ceramics. The maximum permittivity ε' is about 3000, tetragonal — cubic

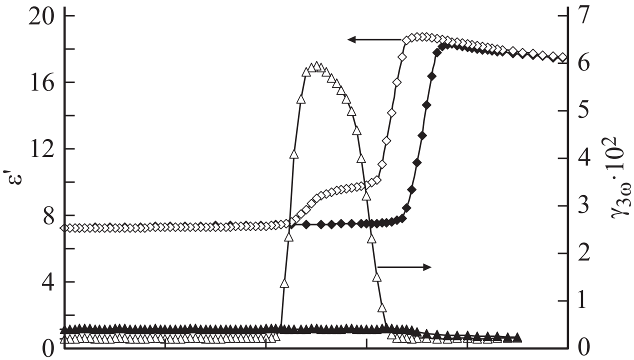

Figure 2. Dependences of permittivity ε' (rhombs) and third harmonic factor $\gamma_{3\omega}$ (triangles) on temperature obtained for KNO_3. Filled symbols — heating, empty symbols — cooling.

phase transition temperature is 123°C in heating and 120°C in cooling, Curie–Weiss constant $C = 0.9 \cdot 10^5\,^\circ$C. Maximum harmonic factors do not exceed ≈ 0.005, which is probably due to a decrease of polarizability of some $BaTiO_3$ ceramics grains as a result of their low volumes [20,21].

Figure 4 shows the temperature dependences of permittivity $\varepsilon'(T)$ and second and third harmonic factors for $BaTiO_3/KNO_3$ nanocomposite. As follows from the curves, when the matrix is filled with KNO_3, its maximum permittivity grows by approx 10%. During heating, two anomalies are observed on $\varepsilon'(T)$ curve. The first of them corresponds to the $BaTiO_3$ ceramics phase transition at 123°C, and the second small anomaly at 130°C is caused by the phase transition in KNO_3. Besides the permittivity growth, an increase of $\operatorname{tg}\delta$ also occurs, which changes from 0.03 for the empty matrix to 0.07 for the filled matrix. According to $\gamma_{2\omega}(T)$ and $\gamma_{3\omega}(T)$, ferroelectric phase of KNO_3 is observed both in heating and cooling. The results are repeated even after long exposure of samples to room temperature, as opposed to KNO_3 in non-polar nanoporous Al_2O_3 matrices [22]. For comparison, Figure 5 shows $\gamma_{3\omega}(T)$ for bulk KNO_3, $BaTiO_3$ and $BaTiO_3/KNO_3$ nanocomposite matrices obtained when $350\,\mathrm{V\cdot cm^{-1}}$ field is applied to the samplle.

The presence of ferroelectric KNO_3 phase in heating is probably associated with the fact that nanoporous $BaTiO_3$ ceramics is polar. Since $BaTiO_3$ ceramics is in the ferroelectric state at a temperature below 123°C, KNO_3 nanoparticles are exposed to the electric field. To describe phase transitions in KNO_3 in terms of the Landau–Ginzburg theory, the expansion of free-energy density F shall include electrical interactions between $BaTiO_3$ and KNO_3 particles ΔF_1. Two order parameters η_1 and η_2 are introduced into the model describing the sequence of two phase transitions in KNO_3 crystals [23,24]:

$$F = F_0 + \frac{1}{2}\alpha_1'\eta_1^2 + \frac{1}{4}\beta_1'\eta_1^4 + \frac{1}{6}\gamma_1'\eta_1^6 + \frac{1}{2}\alpha_2'\eta_1^2 + \frac{1}{4}\beta_2'\eta_1^4 + \frac{1}{6}\gamma_2'\eta_1^6 + a\eta_1\eta_2E - aE^2, \quad (6)$$

where E is the electric field strength, T_{c1} and T_{c2} are the Curie temperatures of the upper and lower phase transitions of KNO_3, respectively, $\alpha_1' = \alpha_1(T - T_{c1})$, $\alpha_2' = \alpha_1(T - T_{c2})$, the rest factors are assumed as constant, independent on temperature. Free energy minimization with respect to the order parameter at $E = 0$ gives the following equations:

$$\frac{\partial F}{\eta_1} = \alpha_1'\eta_1 + \beta_1'\eta_1^3 + \gamma_1'\eta_1^5 = 0;$$

$$\frac{\partial F}{\eta_2} = \alpha_2'\eta_2 + \beta_2'\eta_2^3 + \gamma_2'\eta_2^5 = 0. \quad (7)$$

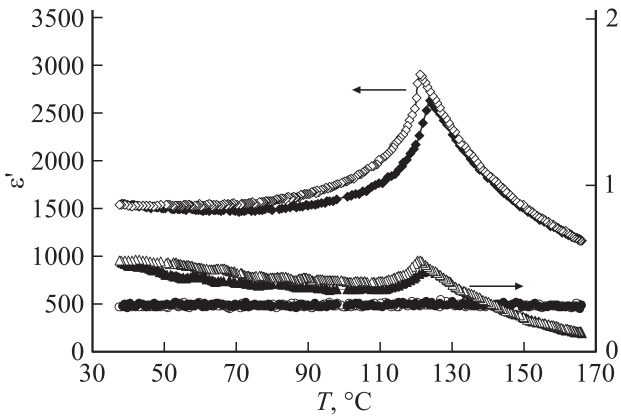

Figure 3. Dependences of permittivity ε' (rhombs) and second (circles) and third (triangles) harmonic factors $\gamma_{3\omega}$ on temperature obtained for porous $BaTiO_3$ ceramics. Filled symbols — heating, empty symbols — cooling.

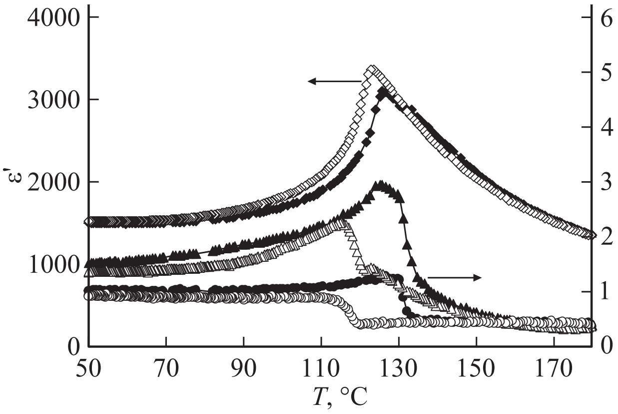

Figure 4. Dependences of permittivity ε' (rhombs) and second (circles) and third (triangles) harmonic factors $\gamma_{3\omega}$ on temperature obtained for $BaTiO_3/KNO_3$ nanocomposite. Filled symbols — heating, empty symbols — cooling.

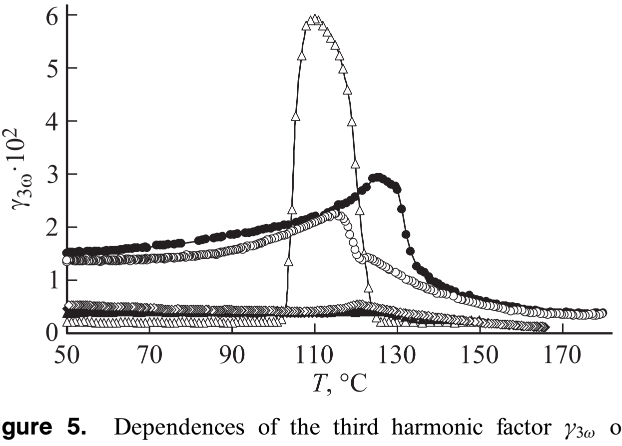

Figure 5. Dependences of the third harmonic factor $\gamma_{3\omega}$ on temperature obtained for KNO_3 (triangles), $BaTiO_3$ ceramics (rhombs) and $BaTiO_3/KNO_3$ nanocomposite (circles). Filled symbols — heating, empty symbols — cooling.

For different factor values in equation (6), the following solutions are available:

$$\eta_1 = \eta_2 = 0; \tag{8}$$

$$\eta_1^2 = \eta_2^2 \neq 0; \tag{9}$$

$$\eta_1^2 = 0; \quad \eta_2^2 \neq 0, \tag{10}$$

where phase I corresponds to equation (8), phase II corresponds to equation (10), and phase III corresponds to equation (9). The spontaneous polarization in phase III is calculated as

$$P_S = \frac{\partial F}{\partial E} = -a\eta_1\eta_2. \tag{11}$$

To describe the properties of KNO_3 nanoparticles in the porous polar matrix, in addition to electrical interactions ΔF_1, the Landau–Ginzburg expansion shall include an additional term ΔF_2 that considers the size effects [25]. The accurate solution of equation (6) is a separate problem and is not addressed herein. However, according to general representations [16], the electric field of the matrix shall facilitate stabilization of the ferroelectric state of KNO_3 in the matrix.

4. Conclusion

According to the findings, for KNO_3 particles in the nanoporous $BaTiO_3$ matrix, polar KNO_3 phase stabilization takes place. Variation of KNO_3 properties may be probably caused by the electric field in $BaTiO_3$ pores that acts on the particles of the introduced substance. Further investigations in this field may enhance our insight into the variation of ferroelectric properties in polar matrices and facilitate the development of new advanced electronic technologies.

Funding

The study was performed under the internal grant of Blagoveshchensk State Pedagogical University.

Conflict of interest

The authors declare that they have no conflict of interest.

References

[1] Q. Li, Y. Zhou. Molecules **28**, 2013 (2023).
[2] Y. Liu, J. Liao, L. Chang, W. Bao. Fuel **311**, 122537 (2022).
[3] B. Xu, S. Li, R. Shi, H. Liu. Sig. Transduct. Target Ther. **8**, 435 (2023).
[4] P.H.C. Camargo, K.G. Satyanarayana, F. Wypych. Mater. Res. **12**, 1, (2009).
[5] C. Tien, E.V. Charnaya, M.K. Lee, S.Y. Sun, S.V. Baryshnikov, D. Michel, W. Böhlmann. Phys. Solid State **46**, 2301 (2004).
[6] A. Sieradzki, J. Komar, E. Rysiakiewicz Pasek, A. Cizman, R. Poprawski. Ferroelectrics **402**, 60 (2010).
[7] P.Yu. Vanina, A. Cizman, E. Rysiakiewicz-Pasek, A. Hoser, A.A. Naberezhnov, A.A. Sysoeva. FTT **60**, 439 (2018). (in Russian).
[8] A.Yu. Milinsky, S.V. Baryshnikov, E.V. Stukova, E.V. Charnaya, I.A. Chernechkin, N.I. Uskova. FTT **63**, 767 (2021). (in Russian).
[9] S.V. Baryshnikov, A.Yu.Milinsky, E.V. Charnaya, I.V. Egorova. FTT **61**, 273 (2019). (in Russian).
[10] S.V. Baryshnikov, A.Y. Milinskiy, E.V. Stukova, E.V. Charnaya, C. Tien, D. Michel. J. Phys.: Condens. Matter **21**, 325902 (2009).
[11] A. Chen, F. Chernow. Phys. Rev. **154**, 493 (1967).
[12] V.V. Deshpande, M.D. Karkhanavala, U.R.K. Rao. J. Thermal Anal. Calorimetry **6**, 613 (1974).
[13] J.K. Nimmo, B.W. Lucas. Acta Cryst. **B32**, 1968 (1976).
[14] E.V. Stukova, S.V. Baryshnikov. Inorganic Mater.: Appl. Res. **2**, 434 (2011).
[15] S. Shimada, T. Aoki. Chem. Lett. **25**, 393 (1996).
[16] M.E. Lines, A.M. Glass. Principles and application of ferroelectrics and related materials. OUP Oxford (2001). 680 p.
[17] H. Guo, A. Baker, J. Guo, A. Clive. ACS Nano **10**, 10606 (2016).
[18] S. Ikeda, H. Kominami, K. Koyama, Y. Wada. J. Appl. Phys. **62**, 3339 (1987).
[19] S.G. Yudin, L.M. Blinov, N.N. Petukhov, S.P. Palto. Pis'ma v ZhETF **70**, 625 (1999). (in Russian).
[20] Z. Zhao, V. Buscaglia, M. Viviani, M. T. Buscaglia, L. Mitoseriu, A. Testino, M. Nygren, M. Johnsson, P. Nanni. Phys. Rev. B **70**, 024107 (2004).
[21] L. Curecheriu, S.-B. Balmus, M. T. Buscaglia, V. Buscaglia, A. Ianculescu, L. Mitoseriu. J. Am. Ceram. Soc. **95**, 3912 (2012).
[22] A.Yu. Milinskii, S.V. Baryshnikov, E.V. Stukova. Nanosci. & Nanotechnology-Asia **12**, 44 (2022).
[23] S.L. Ginzburg. UFN, **38** (490), 1949 (in Russian).
[24] B.A. Strukov, A.P. Levanyuk. Ferroelectric Phenomena in Crystals. Springer, Germany (1998). 303 p.
[25] W.L. Zhong, Y.G. Wang, P.L. Zhang, B.D. Qu. Phys. Rev. B **50**, 698 (1994).

Translated by E.Ilinskaya